reduction of stroke and cardiovascular complications (1). Ca channel blocker is widely used as the blood pressure-lowering agents. However, it has been reported that Ca channels blocker increases heart rate with lowering blood pressure. Among the Ca channels blockers, cilnidipine is known not to increase the heart rate and plasma norepinehrine concentrations in spite of the strong blood pressure lowering effects (2–4). Cilnidipine is a long-acting dihydropyridine calcium channel blocker by inhibiting L-type calcium channels directly associated with vascular tone, and N-type calcium channels related to sympathetic nervous activity (5–7). Whereas cilnidipine inhibits N-type calcium channels, it has not been well established whether cilnidipine decreases the sympathetic nerve activity and increases the parasympathetic nerve activity in the patients with hypertension.

Analysis of spontaneous heart rate and blood pressure variability offers insights into different features of autonomic control of circulation (8), including the arterial baroreflex regulation (9). In this context, heart rate spectral powers in the so-called high-frequency (HF; 0.15–0.40 Hz) and low-frequency (LF; 0.04–0.15 Hz) regions and blood pressure spectra powers in the LF regions have been repeatedly reported to provide relevant information (8, 10–12). The LF power of blood pressure was reported to be increased in parallel with the sympathetic nerve activation (13). Furthermore, the baroreflex control is one of the key mechanisms responsible for the short-term control of blood pressure. Impairment of this reflex has been found in a number of conditions, such as aging (14), heart failure (15), post-myocardial infarction (16), and the impairment of baroreflex sensitivity (BRS) is known as the predictive factor of mortality in hypertension (17). Baroreflex sensitivity was originally assessed by intra-arterial measurement of the change in pulse interval following a pharmacologically induced change in blood pressure. However, for some time now, noninvasive monitoring of blood pressure using finger plethysmography has been available (18), and is an accepted method for tracking beat-to-beat changes in blood pressure (19). Added to this, a further method for measuring BRS has been developed, which assesses spontaneous changes in blood pressure and pulse interval, and does not require pharmacological manipulation of blood pressure-spectral analysis (20,21). However, it has not been determined whether the cilnidipine improves the impaired BRS or not.

Therefore, the aim of the present study was to evaluate the effect of cilnidipine on the sympathetic nerve activity, parasympathetic nerve activity, and BRS in the patients with hypertension. We evaluated the sympathetic and parasympathetic nerve activity using the analysis of systolic blood pressure and heart rate variability, and BRS was measured by the spontaneous sequence method.

Materials and Methods

Subjects

The present study was conducted prospectively on 10 outpatients with hypertension (5 males and 5 females; mean age: 58.6 years; range 44–74 years) whose blood pressure was over 140/90 mmHg. No patients were currently receiving anti-hypertensive medication and all of them were newly diagnosed. Patients with the secondary hypertension were excluded. All studies were performed between 9 and 11 a.m., with each subject examined at the same time of day on each visit to reduce the possible influence of circadian variation in BRS. This study was performed in a quiet room, and every effort was made to keep stimuli to a minimum during the study period. Each subject gave informed

consent to the experimental procedures, which was approved by the ethics committee of our institution.

Measurement of Blood Pressure and Heart Rate

Subjects lay supine, and were rested for a minimum of 15 minutes prior to assessment. Each subject then underwent periods of blood pressure and heart rate monitoring. Blood pressure monitoring was performed using the TaskForce Monitor 3040i (CNSystems, Graz, Austria). The cuff was attached to a finger of the left hand and supported at heart level. Electrocardiogram electrodes were attached to the chest. After a minimum period of 5 minutes, and once a reading of blood pressure and heart rate had stabilized, three consecutive, 5-minute recordings were made of the blood pressure and electrocardiogram tracing. Noninvasive brachial blood pressure readings were taken with an appropriate-sized cuff.

Spectral Analysis for Systolic Blood Pressure and Heart Rate

Spectral analysis was performed using an adaptive auto-regressive model to provide power spectra for both systolic blood pressure (SBP) and R-R interval (RRI). Low Frequency power of SBP was computed by integrating the spectra between 0.04 and 0.15 Hz, and HF power of RRI was computed by integrating the spectra between 0.15–0.40 Hz. Parasympathetic nerve activity was represented by the normalized unit of HF component of RRI (HFnuRRI), and sympathetic nerve activity was represented by the normalized unit of LF component of SBP (LFnuSBP).

Measurement of Baroreflex Sensitivity by Spontaneous Sequence Method

Sequence analysis detected sequences of three or more beats in which there was either an increase in SBP and pulse interval (Up sequence) or a decrease in SBP and pulse interval (Down sequence). Baroreflex sensitivity was estimated as the mean slope of the up sequences (UP BRS), the down sequences (Down BRS), and also the mean slope of all sequences (Sequence BRS) (20,21). Previous reports showed that this protocol measures BRS accurately in animals compared to standard pharmacological techniques (20,21).

Administration of Cilnidipine

Cilnidipine was administered at a dosage of 10–20 mg (10-mg group and 20-mg group) once daily after breakfast according to the guidelines of the treatment with hypertension of the Japanese Society of Hypertension (JSH2004). All the patients were placed on monotherapy with cilnidipine.

Statistical Analysis

All values were expressed as the mean ± SEM. The student's paired *t*-test was used to analyze the changes of variables between pre- and post-treatment with cilnidipine. Differences in variables between the groups were analyzed by one-way ANOVA. A value of $p < 0.05$ was considered statistically significant.

Results

Patients Characteristics

Table 1 shows the baseline characteristics of the two groups. There were no significant differences in age, blood pressure, serum creatinine, and hemoglobin between 10-mg and 20-mg group of cilnidipine. None of the patients had the clinical side effects of cilnidipine.

Effects of Cilnidipine on Blood Pressure and Heart Rate

After the treatment with cilnidipine for 6 months, blood pressure was significantly reduced in all patients, and the effect of blood pressure lowering was significantly greater in 20-mg group than in 10-mg group (Tables 2, 3, and 4). Heart rate was not significantly decreased in both groups after the treatment with cilnidipine (Tables 2, 3, 4).

Effects of Cilnidipine on Sympathetic and Parasympathetic Nerve Activity

After the treatment with cilnidipine for 6 months, LFnuSBP were significantly decreased in both groups (Tables 2 and 3), and the suppressive effects were stronger in the 20-mg group than in the 10-mg group (Table 4). While HFnuRRI was not significantly changed in the 10-mg group (Table 2), it was significantly increased in the 20-mg group (Table 3).

Effects of Cilnidipine on Baroreflex Sensitivity

In the 10-mg group, BRS was not significantly changed between before and after the treatment with cilnidipine (Table 2). However, in the 20-mg group, BRS was significantly improved after the treatment with cilnidipine for 6 months (Table 3).

Table 1
Clinical profile of the patients in 10-mg and 20-mg group

	10-mg Group (n = 5)	20-mg Group (n = 5)	
Age (year)	56 ± 7	59 ± 8	NS
Systolic blood pressure (mmHg)	161 ± 13	157 ±12	NS
Diastolic blood pressure (mmHg)	100 ± 5	98 ± 8	NS
Heart rate (bpm)	80 ± 5	76 ± 6	NS
AST/ALT (IU/L)	26 ± 11/27 ± 13	26 ± 9/28 ± 6	NS
Cr (mg/dL)	0.7 ± 0.2	0.8 ± 0.2	NS
Total cholesterol (mg/dL)	182 ±19	178 ± 22	NS
Triglyceride (mg/dL)	92 ± 33	88 ± 36	NS
LDL cholesterol (mg/dL)	110 ± 14	108 ± 12	NS
HDL cholesterol (mg/dL)	46 ± 7	48 ± 6	NS
Glucose (mg/dL)	89 ± 11	93 ± 10	NS
HbA1c (%)	5.6 ± 0.4	5.5 ± 0.6	NS
BNP (pg/ml)	38 ± 14	32 ± 11	NS
Left ventricular ejection fraction (%)	70 ± 9	72 ± 8	NS
Cardio-thoracic ratio(%)	54 ± 8	51 ± 8	NS

Table 2
Changes in blood pressure, heart rate, and autonomic function in the patients with 10-mg group

	Pretreatment (n = 5)	Cilnidipine 10 mg (n = 5)	P
Systolic blood pressure (mmHg)	161 ± 13	137 ± 13	< 0.05
Diastolic blood pressure (mmHg)	100 ± 5	87 ± 4	< 0.05
Heart rate (bpm)	80 ± 5	76 ± 7	NS
HF-RR (ms2)	102 ± 63	106 ± 58	NS
HFnuRR (%)	39 ± 6	42 ± 6	NS
LF-SBP (mmHg2)	0.7 ± 0.3	0.5 ± 0.5	NS
LFnuSBP (%)	56 ± 5	49 ± 4	< 0.05
Baroreflex sensitivity (ms/mmHg)	14.2 ± 2.6	16.2 ± 4.8	NS

Table 3
Changes in blood pressure, heart rate, and autonomic function in the patients with 20-mg group

	Pretreatment (n = 5)	Cilnidipine 20 mg (n = 5)	P
Systolic blood pressure (mmHg)	157 ± 12	120 ± 13	< 0.05
Diastolic blood pressure (mmHg)	98 ± 8	81 ± 5	< 0.05
Heart rate (bpm)	76 ± 6	73 ± 6	NS
HF-RR (ms2)	92 ± 44	102 ± 66	NS
HFnuRR (%)	39 ± 3	44 ± 2	< 0.05
LF-SBP (mmHg2)	0.6 ± 0.4	0.4 ± 0.3	NS
LFnuSBP (%)	63 ± 6	50 ± 4	< 0.05
Baroreflex sensitivity (ms/mmHg)	13.6 ± 2.9	20.2 ± 2.1	< 0.05

Table 4
Degree of changes in blood pressure, heart rate and autonomic function in the patients with 10-mg and 20-mg group

	Cilnidipine 10 mg (n = 5)	Cilnidipine 20 mg (n = 5)	P
Systolic blood pressure	−15%	−24%	< 0.05
Diastolic blood pressure	−13%	−17%	< 0.05
Heart rate	−5%	−4%	NS
HFnuRR	+7%	+13%	< 0.05
LFnuSBP	−12%	−12%	< 0.05
Baroreflex sensitivity	+14%	+49%	< 0.05

Discussion

In the present study conducted among patients with essential hypertension, cilnidipine produced a significant reduction in blood pressure with the inhibition of sympathetic nerve activity and the improvement of impaired baroreflex control. This study was the first to report that cilnidipine treatment achieved the inhibition of sympathetic nerve activity and the improvement of the impaired baroreflex control in the patients with hypertension. These results suggest that cilnidipine is preferable for the treatment with hypertension among the Ca channel blockers.

Epidemiological studies have demonstrated that a higher heart rate is associated with a long-term risk of cardiovascular mortality, independent of other cardiac risk factors (22). Therefore, anti-hypertensive drugs that do not increase the heart rate would seem to be preferable. It has been reported that the treatment with short-acting Ca channel blockers may not prevent cardiovascular disease (23,24). Accordingly, long-lasting Ca channel blockers that exert less influence on the sympathetic nervous system are now recommended for the treatment of hypertension. Amlodipine and cilnidipine, which were known as long-acting Ca channel blockers, were reported not to increase heart rate. Eguchi et al. (27) reported that cilnidipine did not cause reflex tachycardia, and that cilnidipine, but not amlodipine, significantly decreased the ambulatory BP level without causing an increase in heart rate. In this study, cilnidipine did not increase heart rate, and caused a significant decrease in the LFnuSBP, as the marker of the sympathetic nerve activity. Our results of the sympatho-inhibitory effects of cilnidipine were similar to the previous reports which calculated the sympathetic nerve activity by other methods. From these results, cilnidipine is considered to be the preferable drug with the sympatho-inhibtory effect among the Ca channel blockers.

In this study, BRS was improved in the patients with hypertension treated with high-dose cilnidipine. A previous study reported that BRS values calculated by sequence analysis had reasonable reproducibility when up and down sequences were combined (25), and we measured the BRS by sequence analysis. It has been reported that BRS is impaired in the patients with hypertension (17,26–29), and that BRS is the predictive factor of mortality and cardiovascular events (17). The results of this study suggest that cilnidipine is preferable for the treatment of hypertension among the Ca channel blockers. Previous studies suggested BRS measured by the sequence method was impaired in the patients with hypertension (5–12 ms/mmHg) (27–29), and BRS obtained in this study was considered to be higher compared to that in those previous studies. This difference may be due to the patients' characteristics in this study. The patients in this study had no complications and their hypertension was in early stages.

The mechanisms in which cilnidipine inhibits the sympathetic nerve activity may be due to suppressing the release of catecholamines from sympathetic nerve endings by blocking the N-type calcium channels distributed widely in sympathetic nerves (30). Recent studies have demonstrated the beneficial effect of cilnidipine on cardiac sympathetic nerve activity and cardiovascular morbidity (31–33). Sakata, Yoshida, and Obayashi reported that cilnidipine suppressed cardiac sympathetic overactivity while amlodipine had little suppressive effect (32). The effect of cilnidipine on heart rate might be due to not only long-acting effects but also to a reduction in sympathetic nerve activity. The mechanisms in which cilnidipine improved the BRS has not been determined in this study. Our previous study in animal models indicated that sympatho-inhibition causes the improvement of BRS in hypertensive model rats (26). Further clinical studies are necessary.

There are several limitations in this study. First, this study was a small-size, nonrandomized study. To establish the sympatho-inhibitory effect and improvement of BRS of cilnidipine, a randomized study is required. Second, the ages of the patients in this study were relatively young, and none of them had organ damage due to hypertension. Whether the treatment with cilnidipine causes the beneficial effects in this study in the older and complicated patients with hypertension has not been determined. Third, we determined the effects of cilnidipine on autonomic function for only 6 months, and only at two points, before and after 6 months. The blood pressure-lowering effect of cilnidipine is determined in several days after the initiation of administration (3). In the present study, we examined the effects of cilnidipine on the autonomic function at only two points pre—administration and after 6 months. From the results of the present study, we have not determined whether the mechanisms of the action of cilnidipine is similar between several days and 6 months after the initiation of cilnidipine. Furthermore, the effects of cilnidipine on the autonomic function for longer periods must be determined.

Conclusion

The treatment with cilnidipine for essential hypertension produced a significant reduction in blood pressure with the inhibition of sympathetic nerve activity and the improvement of impaired baroreflex control. These results suggest that cilnidipine is preferable for the treatment of hypertension among the Ca channel blockers.

Acknowledgments

This work was supported by a Grant-in-Aid for Scientific Research from the Japan Society for the Promotion of Science (B19390231), and in part, by the Health and Labor Sciences Research Grant for Comprehensive Research in Aging and Health Labor and Welfare of Japan. We thank all medical staff of the Department of Cardiovascular Medicine of Kyushu University Hospital, our colleagues, friends, parents, and special thanks to my co-author, Dr. Satomi Konno.

Declaration of Interest

The authors report no conflicts of interest. The authors alone are responsible for the content and writing of the paper.

References

1. Staessen JA, Wang JG, Thijs L. Cardiovascular prevention and blood pressure reduction: a quantitative overview updated until March 2003. *J Hypertens.* 2003;21:1055–1076.
2. Yoshimoto R, Hashiguchi Y, Dohmoto H, Hosono M, Iida H, Fujiyoshi T, Ikeda K, Hayashi Y. Effects of a new dihydropyridine derivative, FRC-8653, on blood pressure in conscious spontaneously hypertensive rats. *J Pharmacobio Dyn* 1992;15:25–32.
3. Tominaga M, Phya Y, Tsukashima A, Kobayashi K, Takata Y, Koga T, Yamashita Y, Fujishima Y, Fujishima M. Ambulatory blood pressure monitoring in patients with essential hypertension treated with a new calcium antagonist, cilnidipine. *Cardiovasc Drugs Ther* 1997;11:43–48.
4. Hosono M, Fujii S, Hiruma T, Watanabe K, Hayashi Y, Ohnishi H, Takata Y, Kato H. Inhibitory effect of cilnidipine on vascular sympathetic neurotransmission and subsequent vasoconstriction in spontaneously hypertensive rats. *Jpn J Pharmacol* 1995;69:127–134.

5. Oike M, Inoue Y, Kitamura K, Kuriyama H. Dual action of FRC8653, a novel dihydropyridine derivative, on the Ba2+ current recorded from the rabbit artery. *Circ Res* 1990;57:993–1006.
6. Fujii S, Kameyama K, Hosono M, Hayashi Y, Kitamura K. Effect of cilnidipine, a new dihidropyrydine Ca++ channel antagonist, on N-type Ca++ channel in rat dorsal root ganglion neurons. *J Pharmacol Exp Ther* 1997;280:1184–1191.
7. Uneyama H, Takahara A, Dohmoto H, Yoshimoto R, Inoue K, Akaike N. Blockade of N-type Ca++ current by cilnidipine (FRC-8653) in acutely dissociated rat sympathetic neurons. *Br J Pharmacol* 1997;122:37–42.
8. Mancia G, Parati G, Castiglioni P, Di Rienzo M. Effect of sinoaortic deervation on frequency-domain estimates of baroreflex sensitivity in conscious cats. *Am J Physiol* 1999;276:H1987–H1993.
9. Laude D, Elghozi JL, Girard A, Bellard E, Bouhaddi M, Castiglioni P, Cerutti C, Cividjian A, Di Rienzo M, Fortrat JO, Janssen B, Karemaker JM, Leftheriotis G, Parati G, Persson PB, Porta A, Quintin L, Regnard J, Rudiger H, Stauss HM. Comparison of various techniques used to estimate spontaneous baroreflex sensitivity. *Am J Physiol* 2004;286:R226–R231.
10. Task Force of the European Society of Cardiology and the North American Society of Pacing and Electrophysiology. Heart rate variability: standards of measurement, physiological interpretation, and clinical ise. *Eur Heart J* 1996;17:354–381.
11. Lucini D, Meta GS, Malliani A, Pagani M. Impairment in cardiac autonomic regulation preceding arterial hypertension in humans: insights from spectral analysis of beat-by-beat cardiovascular variability. *Circulation* 2002;106:2673–2679.
12. Radaelli A, Perlangeli S, Cerutti MC, Mircoli L, Mori I, Boselli K, Bonaita M, Terzoli L, Candotti G, SIgnorini G, Ferrari AU. Altered blood pressure variability in patients with congestive heart failure. *J Hypertens* 1999;17:1905–1910.
13. Castiglioni P, Di Rienzo M, Veicsteinas A, Parati G, Merati G. Mechanisms of blood pressure and heart rate variability: an insight from low-level paraplegia. *Am J Physiol* 2007;292: R1502–R1509.
14. Latinen T, Hartikainen J, Vanninen E, Niskanen L, Geelen G, Lansimies E. Age and gender dependency of baroreflex sensitivity in healthy subjects. *J Appl Physiol* 1998;84:576–583.
15. Mortara A, La Rovere MT, Pinna GD, Prpa A, Maestri R, Fedo O, Pozzoli M, Opasich C, Tavazzi L. Arterial baroreflex modulation of heart rate in chronic heart failure: clinical and hemodynamic correlates and prognostic implications. *Circulation* 1997;96:3450–3458.
16. Farrell TG, Odemuyiwa O, Bashir Y, Gripps TR, Malik M, Ward DE, Camm AJ. Prognostic value of baroreflex sensitivity testing after acute myocardial infarction. *Br Heart J* 1992;67: 129–137.
17. Hesse C, Charkoudian N, Liu Z, Joyner MJ, Eisenach JH. Baroreflex sensitivity inversely correlates with ambulatory blood pressure in healthy normotensive humans. *Hypertension* 2007;50: 41–46.
18. Imholz BP, Wielong W, Langewouters GJ, van Montfrans GA. Continuous finger arterial pressure: utility in the cardiovascular laboratory. *Clin Auton Res* 1991;11:43–53.
19. Imholz BP, Wieling W, van Montfrans GA, Wesseling KH. Fifteen years experience with finger arterial pressure monitoring: assessment of the technology. *Cardiovasc Res* 1998;38:605–616.
20. Waki H, Kasparov S, Wong LF, Murphy D, Shimizu T, Paton JFR. Chronic inhibition of eNOS activity in nucleus tractus solitarii enhances baroreceptor reflex in conscious rats. *J Physiol* 2003;546:233–242.
21. Waki H, Katahira K, Polson JW, Kasparov S, Murphy D, Paton JFR. Automation of analysis of cardiovascular autonomic function from chronic measurements of arterial pressure in conscious rats. *Exp Physiol.* 2006;91:201–213.
22. Gillman MW, Kannel WB, Belanger A, D'Agostuno RB. Influence of heart rate on mortality among patients with hypertension: the Framingham Study. *Am Heart J* 1993;125:1148–1154.
23. Furberg CD, Psaty BM, Meyer JV. Nifedipine: Dose-related increase in mortality in patients with coronary heart disease. *Circulation* 1995;92:1326–1331.
24. Psaty BM, Heckbert SR, Koepsell TD. The risk of myocardial infarction associated with antihypertensive drug therapies. *JAMA* 1995;274:620–625.

25. Johnson P, Shore A, Potter J, Panerai R, James M. Baroreflex sensitivity measured by spectral and sequence analysis in cerebrovascular disease. *Clin Auton Res* 2006;16:270–275.
26. Kishi T, Hirooka Y, Kimura Y, Sakai K, Ito K, Shimokawa H, Takeshita A. Overexpression of eNOS in RVLM improves impaired baroreflex control of heart rate in SHRSP. *Hypertension* 2003;41:255–260.
27. Eguchi K, Tomizawa H, Ishikawa J, Hoshide S, Pickering TG, Shimada K, Kario K. Factors associated with baroreflex sensitivity: associated with morning blood pressure. *Hypertens Res* 2007;30:723–728.
28. Milan A, Caserta MA, Del Colle S, Dematteis A, Morello F, Rabbia F, Mulatero P, Pandian NG, Veglio F. Baroreflex sensitivity correlates with left ventricular morphology and diastolic function in essential hypertension. *J Hypertens* 2007;25:1655–1664.
29. Eguchi K, Tomizawa H, Ishikawa J, Hoshide S, Fukuda T, Numao T, Shimada K, Kario K. Effects of new calcium channel blocker, azelnidipine, and amlodipine on baroreflex sensitivity and ambulatory blood pressure. *J Cardiovasc Pharmacol* 2007;49:394–400.
30. Yamagishi T. Beneficial effect of cilnidipine on morning hypertension and white-coat effect in patients with essential hypertension. *Hypertens Res* 2006;29:339–344.
31. Sakaki T, Naruse H, Masai M. Cilnidipine as an agent to lower blood pressure without sympathetic nervous activation as demonstrated by iodine-123 metaiodobenzyl guanidine imaging in rat heart. *Ann Nucl Med* 2003;17:321–326.
32. Sakata K, Yoshida H, Obayashi K. Comparative effect of cilnidipine and quinapril on left ventricular mass in mild essential hypertension. *Drugs Exp Clin Res* 2003;29:117–123.
33. Nagai H, Minatoguchi S, Chen XH. Cilnidipine, an N+L-type dihydropyridine Ca channel blocker, suppresses the occurrence of ischemia/reperfusion arrhythmia in a rabbit model of myocardial infarction. *Hypertens Res* 2005;28:361–368.

Therapeutic Neovascularization by Nanotechnology-Mediated Cell-Selective Delivery of Pitavastatin Into the Vascular Endothelium

Mitsuki Kubo, Kensuke Egashira, Takahiro Inoue, Jun-ichiro Koga, Shinichiro Oda, Ling Chen, Kaku Nakano, Tetsuya Matoba, Yoshiaki Kawashima, Kaori Hara, Hiroyuki Tsujimoto, Katsuo Sueishi, Ryuji Tominaga, Kenji Sunagawa

Objective—Recent clinical studies of therapeutic neovascularization using angiogenic growth factors demonstrated smaller therapeutic effects than those reported in animal experiments. We hypothesized that nanoparticle (NP)-mediated cell-selective delivery of statins to vascular endothelium would more effectively and integratively induce therapeutic neovascularization.

Methods and Results—In a murine hindlimb ischemia model, intramuscular injection of biodegradable polymeric NP resulted in cell-selective delivery of NP into the capillary and arteriolar endothelium of ischemic muscles for up to 2 weeks postinjection. NP-mediated statin delivery significantly enhanced recovery of blood perfusion to the ischemic limb, increased angiogenesis and arteriogenesis, and promoted expression of the protein kinase Akt, endothelial nitric oxide synthase (eNOS), and angiogenic growth factors. These effects were blocked in mice administered a nitric oxide synthase inhibitor, or in eNOS-deficient mice.

Conclusions—NP-mediated cell-selective statin delivery may be a more effective and integrative strategy for therapeutic neovascularization in patients with severe organ ischemia. (***Arterioscler Thromb Vasc Biol.* 2009;29:796-801.)

Key Words: nanotechnology ■ drug delivery system ■ statin ■ therapeutic neovascularization

Restoration of tissue perfusion in patients with critical ischemia attributable to coronary artery disease and peripheral artery disease is a major therapeutic goal. Recently, double-blind placebo-controlled clinical trials designed to induce neovascularization by administering exogenous angiogenic growth factors failed to demonstrate a clinical benefit and produced some undesired side effects.[1,2] These nonoptimal clinical results were in contrast to the results obtained in animal experiments and small open-label clinical trials.[3,4] The disappointing results of the clinical trials of therapeutic angiogenesis may be attributable in part to less effective transfection of the genetic materials or the rapid washout of proteins. In addition, because the involvement of multiple endogenous angiogenic growth factors is required for the development of functional collaterals,[5,6] the strategy of simple intramuscular injection of an exogenous angiogenic growth factor is limited. A high local concentration of angiogenic growth factors increases the risks of edema,[3,7] angioma-like capillary formation,[7–9] atherosclerosis after vascular injury,[10–13] and tumor-angiogenesis.[7,8] A controlled drug delivery system (DDS) for an integrative approach to therapeutic neovascularization would be more favorable.

To address this challenge, we developed a novel nanoparticle (NP)-mediated DDS, formulated from the bioabsorbable polylactide/glycolide copolymer (PLGA).[14] The PLGA NP offers the advantages of safety, delivery of encapsulated drugs into the cellular cytoplasm, and slow cytoplasmic drug release.[14,15] PLGA NP are effectively and rapidly taken up by vascular endothelial cells in vitro.[16] To our knowledge, however, no prior studies have examined whether PLGA NPs are useful as an endothelial cell-selective DDS in vivo.

We hypothesized that HMG-CoA reductase inhibitors, so-called statins, are appropriate candidate drugs for this integrative approach, because statins have a variety of pleiotropic vasculoprotective effects that are independent of their lipid-lowering activity.[17] Statins increase the angiogenic activity of mature endothelial cells as well as that of endothelial progenitor cells (EPCs)[18,19] and augment collateral growth in ischemic heart and limb in experimental animals.[20,21] In addition, statins attenuate atherosclerosis formation[22,23] and have little potential risk of tumor angiogenesis in contrast to angiogenic growth factors.[24] Most of these beneficial effects of statin on therapeutic neovascularization, however, were observed after daily administration of high doses,[18–21] which

Received December 9, 2008; revision accepted March 16, 2009.

From the Department of Cardiovascular Medicine (M.K., K.E., T.I., J.K., L.C., K.N., T.K., K. Sunagawa), Surgery (S.O., R.T.), and Pathology (K. Sueishi), Graduate School of Medical Sciences, Kyushu University, Fukuoka, Japan; the School of Pharmaceutical Science (Y.K.), Aichi Gakuin University, Aichi, Japan; and Hosokawa Powder Technology Research Institute (K.H., H.T.), Osaka, Japan.

Correspondence to Kensuke Egashira, MD, PhD, Department of Cardiovascular Medicine, Graduate School of Medical Science, Kyushu University, 3-1-1, Maidashi, Higashi-ku, Fukuoka 812-8582, Japan. E-mail egashira@cardiol.med.kyushu-u.ac.jp

Arterioscler Thromb Vasc Biol is available at http://atvb.ahajournals.org DOI: 10.1161/ATVBAHA.108.182584

may lead to serious adverse side effects in a clinical setting. Because vascular endothelium plays a primary role in the pathogenesis of ischemia-induced neovascularization, we hypothesized that NP-mediated cell-selective delivery of statins to the vascular endothelium would more effectively and integratively induce therapeutic neovascularization.

The major aim of this study was to test the hypothesis that selective NP-mediated delivery of statins to endothelial cells can be an integrative approach to enhance therapeutic neovascularization. We used a murine model of hindlimb ischemia to examine, (1) whether PLGA NPs are delivered selectively to vascular endothelial cells in ischemic tissues; and (2) whether NP-mediated delivery of statin is useful for increasing therapeutic neovascularization.

Materials and Methods

Preparation of PLGA NPs

Anionic PLGA NPs encapsulated with fluorescein isothiocyanate (FITC) or pitavastatin were prepared by a previously reported emulsion solvent diffusion method in purified water. The diameter of the PLGA NPs was 196±29 nm. The PLGA NPs had a negative surface charge (-15±10 mV). The FITC- and pitavastatin-loaded PLGA NPs contained 5% (wt/vol) FITC and 5% (wt/vol) pitavastatin, respectively. Additional details are provided in the supplemental information (please see http://atvb.ahajournals.org.).

Intracellular Uptake and Intracellular Distribution of NPs

Human umbilical vein endothelial cells (HUVECs) were obtained and cultured in EGM-2. Human skeletal muscle cells (SkMCs) were obtained and cultured in SkGM. Additional details can be found in the supplemental information.

Angiogenesis Assay of Human Endothelial Cells

Angiogenesis assay of human endothelial cells was tested using a 2-dimensional Matrigel assay. Additional details are provided in the supplemental information.

Animal Preparation and Experimental Protocol

Male 8-week-old C57BL/6J wild-type mice were used. After anesthesia, we induced unilateral hindlimb ischemia in the mice as previously described.[25] Immediately after the induction of ischemia, animals were randomly divided into 4 groups; a control no treatment group and the remaining groups received intramuscular injections of FITC-NPs (NP group), pitavastatin at 0.4 mg/kg (statin only group), or pitavastatin-NPs containing 0.4 mg/kg pitavastatin (statin-NP group) into the left femoral and thigh muscles. Biochemical parameters listed in supplemental Table I were measured 3, 7, and 14 days after treatment. Additional details are provided in the supplemental information.

Limb blood flow measurements were performed using a laser Doppler perfusion imaging (LDPI) analyzer (Moor Instruments). The LDPI index was expressed as the ratio of the LDPI signal in the ischemic limb compared to that in the normal limb.[25]

Histological and Immunohistochemical Analyses

Histological and immunohistochemical evaluation was performed. To determine capillary and arteriolar density, cross sections were stained with anti-mouse platelet endothelial cell adhesion molecule (PECAM)-1 antibody (CD31) and α-smooth muscle actin (α-SMA), respectively. Additional details are provided in the supplemental information.

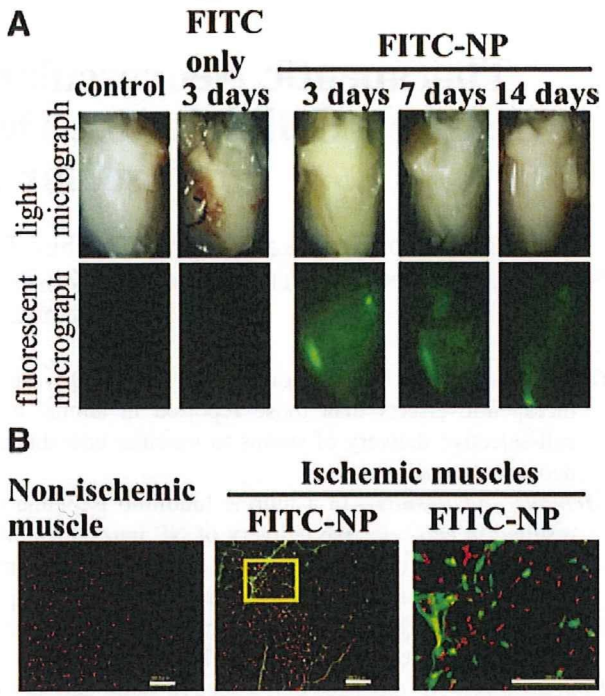

Figure 1. A, Representative light and fluorescent stereomicrographs of gastrocnemius muscles from control nonischemic hindlimb and from ischemic hindlimb. B, Fluorescent micrographs of cross-sections from nonischemic muscle with no injection, ischemic muscles 14 days after the injection of FITC-NP, and expanded view of boxed area of middle panel. Scale bars: 100 μm.

Western Blotting

Protein expression of Akt, eNOS, VEGF, FGF-2, and MCP-1 was examined 7 days after the induction of hindlimb ischemia. Additional details are provided in the supplemental information.

Flow Cytometric Analyses of EPC Mobilization

Peripheral blood was obtained from mice 7 and 14 days after hindlimb ischemia and analyzed with a FACS Caliber flow cytometer (Becton Dickinson). Additional details are provided in the supplemental Information.

Measurements of Statin Concentration in Serum and Muscle Tissue

Statin concentration in serum and muscle were measured at predetermined time points using a column-switching high performance liquid chromatography system. Additional details are provided in the supplemental information.

Statistical Analysis

Data are expressed as means±SEM. The statistical analysis was assessed using analysis of variance and multiple comparison tests. Probability values less than 0.05 were considered to be statistically significant.

Results

Cell-Selective Delivery of NPs In Vivo

Cellular distribution of FITC was examined 3, 7, and 14 days after intramuscular injection of FITC-NP or FITC only. On day 3 postinjection, strong FITC signals were detected only in FITC-NP injected ischemic muscle, whereas no FITC signals were observed in control nonischemic muscle or in ischemic muscle injected with FITC only (Figure 1A). The FITC

signals were localized predominantly in the capillaries and arterioles. FITC signals were also detected in myocytes at this time point. These data suggest that NP solution might distribute to intra- and extracellular spaces of ischemic skeletal muscle tissues immediately after intramuscular injection of NPs, and then the NP was uptaken by cells in injected muscles (endothelial cells, smooth muscle cells, myocytes, etc) or retained in extracellular spaces at this early time point.

On days 7 and 14, FITC signals remained localized predominantly in capillaries and arterioles (Figure 1B). Immunofluorescent staining revealed FITC signals localized mainly in endothelial cells positive for CD31, a marker of angiogenesis, in FITC-NPs injected ischemic muscle 14 days postischemia (supplemental Figure I). In contrast, no FITC signals were observed in myocytes. FITC signals were not detected in contralateral nonischemic hindlimb or in remote organs (liver, spleen, kidney, and heart) at any time point (data not shown).

Cellular Delivery of NPs Into Vascular Endothelial Cells Versus Skeletal Myocytes In Vitro

Cellular uptake of NPs was examined in HUVECs and SkMCs after incubation with FITC-NPs for 1 hour. The number of FITC-positive cells was greater among HUVECs than among SkMCs (supplemental Figure IIA). An inhibitor of clathrin-mediated endocytosis, chlorpromazine (CPZ), did not affect the magnitude of cellular FITC signals in SkMCs, but reduced the magnitude in HUVECs (supplemental Figure IIB). Long-term cell culture after 1-hour incubation with FITC-NPs revealed cellular FITC signals in HUVECs on days 3 and 7 postincubation (supplemental Figure IIC). In contrast, no FITC signal was detected in SkMC (data not shown).

Effects of Statin-NP on Ischemia-Induced Neovascularization

Treatment with statin-NP that contains pitavastatin at 0.4 mg/kg, but not with FITC-NP or statin only, significantly increased blood flow recovery on days 7 and 14 (Figure 2A and 2B). The beneficial effects of statin-NP were not associated with significant changes in serum biochemical markers (supplemental Table I), but angiogenesis and arteriogenesis were significantly increased (Figure 2C). Examination of hematoxylin-eosin-stained sections revealed no abnormal histopathologic findings (inflammation and fibrosis) among the 4 groups (data not shown). There was no significant difference in muscle fiber density among the 4 groups (data not shown).

Single intramuscular injection of nonnanoparticulated soluble pitavastatin at doses of 4 and 20 mg/kg exerted no effect on blood perfusion after hindlimb ischemia (supplemental Figure IIIA). Oral daily administration of pitavastatin at 0.4 mg/kg did not increase blood flow recovery, but pitavastatin at 1.0 and 10 mg/kg significantly increased blood flow recovery on day 14 (supplemental Figure IV).

Systemic daily administration of statins is reported to increase EPC mobilization,[18,26] but the EPC number in the circulating blood was not increased in the present study (supplemental Figure IIIB and IIIC). No therapeutic effects of

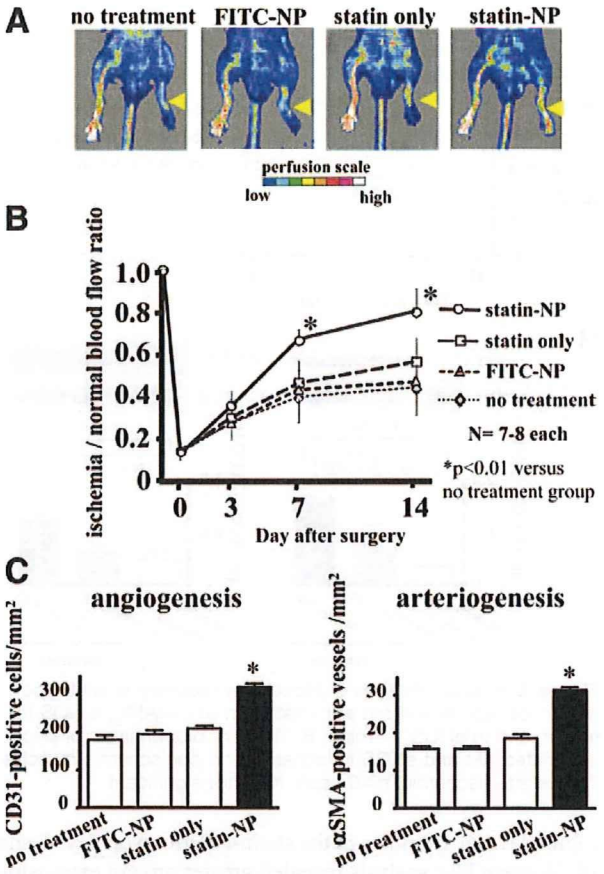

Figure 2. A, Representative laser Doppler perfusion imaging at 14 days postischemia. Arrow indicates ischemic limb. B, Quantification of blood flow recovery. C, Quantitative analysis of angiogenesis and arteriogenesis. n=4 each. *$P<0.01$ vs no treatment group.

statin-NP were observed in wild-type mice administered L-NAME or in eNOS$^{-/-}$ mice (Figure 3A), suggesting that eNOS-related signals are involved in the mechanism of statin-induced enhancement of ischemia-induced neovascularization (supplemental Figure V). Treatment with statin-NP increased both phosphorylated eNOS and serine-threonine specific protein kinase (Akt) in ischemic muscles compared with nonischemic control and nontreated ischemic muscles at 7 days of treatment (Figure 3B). Immunohistochemistry revealed that the increased eNOS and Akt activities were localized mainly in microvascular endothelial cells (supplemental Figure VI).

Effect of Statin-NP on Endogenous Angiogenic Growth Factor Expression

Immunohistochemistry was performed to examine the cellular localization of angiogenic growth factors in control and statin-NP groups. On day 3, immunostaining for both vascular endothelial growth factor (VEGF) and fibroblast growth factor-2 (FGF-2) was observed in skeletal myocytes and blood vessels (supplemental Figure VII). On days 7 and 14, the immunostaining intensity markedly decreased in skeletal myocytes and blood vessels in the control group. In contrast, positive immunostaining was observed in endothelial cells of

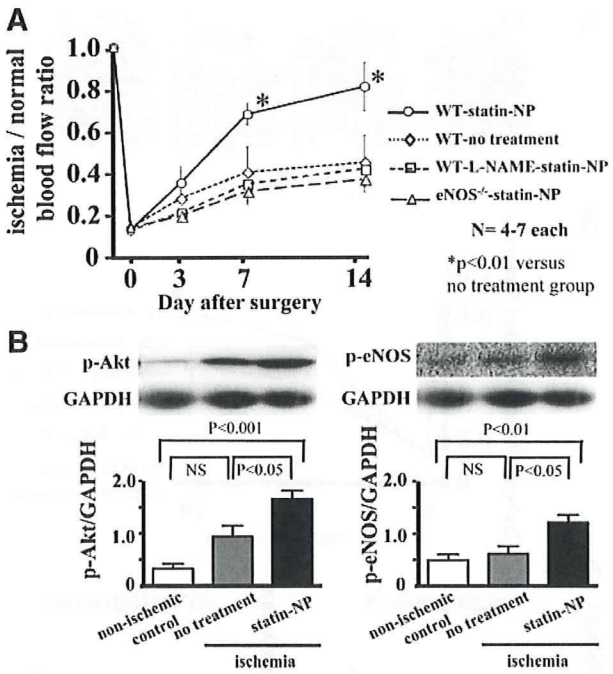

Figure 3. A, Quantification of blood flow recovery in wild-type (WT) mice with or without administration of L-NAME, a NOS inhibitor, and in $eNOS^{-/-}$ mice. B, Western blot analysis of phosphorylated Akt and eNOS in ischemic and nonischemic muscles 7 days after ischemia. n=6 each. NS=not significant.

capillaries and arterioles in the statin-NP group on days 7 and 14. Western blot analysis revealed greater protein expression of VEGF, FGF-2, and monocyte chemotactic protein-1 (MCP-1) in ischemic muscle in the statin-NP group than in the no treatment group 7 days after hindlimb ischemia (Figure 4). Interestingly, the increased expression of such angiogenic growth factors by treatment with statin-NP was blunted in mice administered chronically with L-NAME.

Effects of Statin-NP on Angiogenic Capacity of Human Endothelial Cells In Vitro

Cotreatment with statin or statin-NP increased angiogenic activity in HUVECs. The angiogenic activity of statin-NP was greater than that of 10 nmol/L statin only (supplemental Figure VIIIA). Pretreatment with statin only (24-hour incubation of HUVECs with statin) had no angiogenic effects at any dose. In contrast, pretreatment with statin-NP induced significant angiogenic effects at 1 and 10 nmol/L compared with the no-treatment control group (supplemental Figure VIIIB).

Serum and Tissue Concentrations of Statin

Tissue concentrations of pitavastatin were greater in skeletal muscles injected with statin-NPs than in those injected with statin 6 and 24 hours after intramuscular administration, whereas serum levels of pitavastatin were comparable between the 2 groups (supplemental Table II). The drug was not detected in serum 1 and 3 days after injection.

Discussion

The application of nanotechnology-based drug delivery is expected to have a major impact on the development of

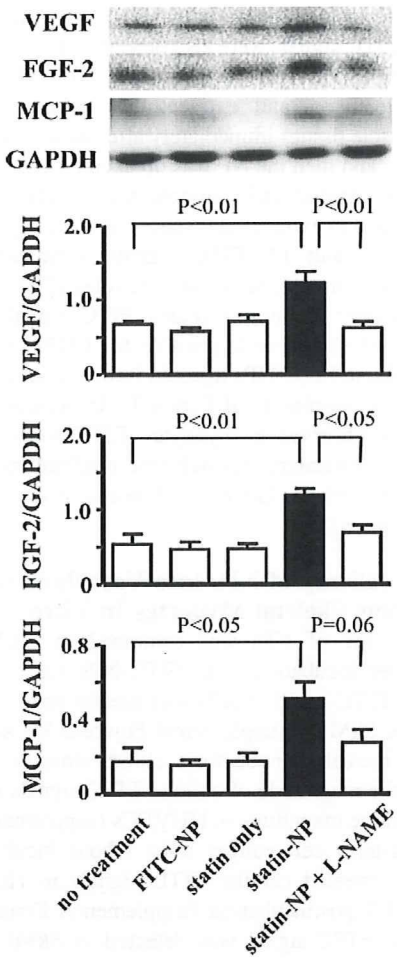

Figure 4. Effects of statin-NP on expression of VEGF, FGF-2, and MCP-1 in ischemic muscle. Densitometric analysis of protein expression in ischemic muscles 7 days after ischemia. Quantitative evaluation was expressed as a ratio of VEGF, FGF-2, and MCP-1 to GAPDH. n=6 each.

innovative medicines. In the present study, selective NP-mediated delivery of statin to vascular endothelial cells increased neovascularization and improved tissue perfusion in a murine model of hindlimb ischemia, indicating that this novel cell-selective delivery system is feasible for therapeutic neovascularization.

The most novel finding of this study is that FITC signals were localized mainly in the vascular endothelium 7 and 14 days after injection of FITC-NP into ischemic skeletal muscles in vivo. Several factors might be involved in mechanisms of the cell-selective delivery of the NP at later time points. First, increased endocytosis of NP in the endothelium may be involved, which is based on our present experiments with CPZ, an inhibitor of clathrin-mediated endocytosis. In addition, 1-hour incubation with FITC-NP resulted in long-term and stable retention of NP in the human endothelial cells, but not in skeletal myocytes in vitro. Second, decreased exocytosis of the endothelium in the presence of ischemia might also be involved. Third, after cellular delivery of NP via endocytosis, rapid escape of the NP from the endosomal compartment to the cytoplasmic compartment may lead to

sustained intracellular drug delivery and good efficacy. The NP is likely retained in the cytoplasm where release of the encapsulated drug occurs slowly in conjunction with the hydrolysis of PLGA.[15] Overall, the nanotechnology platform for cell-selective delivery to the vascular endothelium using NP may be useful as an innovative strategy for therapeutic neovascularization and other intractable diseases.

Another important feature of this study is that a single administration of statin-NP containing pitavastatin (0.4 mg/kg) into vascular endothelial cells effectively increased therapeutic neovascularization with no serious side effect in murine model of hindlimb ischemia. Sata et al[24] reported that systemic daily administration of pitavastatin (1 mg/kg per day × 49 days=49 mg/kg) has significant therapeutic effects in mice with hindlimb ischemia. In the present study, we confirmed the study of Sata et al[24] by showing that oral daily administration of pitavastatin for 14 days (1 and 10 mg/kg per day × 14=14 and 140 mg/kg, respectively) had significant therapeutic effects, as did statin-NP (0.4 mg/kg). Therefore, our NP-mediated delivery system seems to be as effective at an approximately 100-times lower dose than the cumulative systemic dose. Furthermore, measurement of the tissue and serum concentrations of pitavastatin confirmed the effective local retention of statin-NPs in ischemic skeletal muscles in vivo. NP-mediated delivery of pitavastatin accelerated angiogenic activity of human endothelial cells in vitro. Therefore, it is possible that after NP-mediated endothelial delivery, pitavastatin was slowly released from the NPs into the cytoplasm along with PLGA hydrolysis, resulting in significant therapeutic effects.

Clearly, the therapeutic neovascularization induced by statin-NPs resulted from the pleiotropic effects, because pitavastatin-NPs had no effect on serum lipid levels. Our experiments with mice treated with a NOS inhibitor and $eNOS^{-/-}$ mice support the essential role of the eNOS pathway in the mechanism underlying the therapeutic effects of NP-mediated cell-selective delivery of statin. Consistent with the results of other investigators,[18,20,21,26] we demonstrated that pitavastatin-NP increased the activity of vascular eNOS and PI3K/Akt (as shown in supplemental Figure V) in association with an increased expression of endogenous multiple angiogenic growth factors that are involved in angiogenesis (VEGF) and arteriogenesis (FGF-2, MCP-1).[27] These therapeutic effects afforded by the NP-mediated cell-selective delivery of statin were not associated with a further increase in circulating EPC. Intramuscular injection of soluble pitavastatin alone at high doses (4 and 20 mg/kg) has no therapeutic effect, suggesting a specific advantage of endothelial cell selective delivery of pitavastatin by the PLGA NP formulation. These findings suggest that pitavastatin-NP acted locally on ischemic vascular endothelium to induce therapeutic neovascularization and are consistent with the notion that NP-mediated endothelial cell-selective delivery of statin produces a well-harmonized integrative system to form functionally mature collaterals via controlled expression of endogenous multiple angiogenic growth factors and signals, allowing for a more effective model for an integrative approach to therapeutic neovascularization.

There is a major limitation to the present study. First, we examined only a single dose of statin-NPs. It is difficult to obtain a dose-response relationship of this NP system in small animals. For translation of our present findings into clinical medicine, further studies are needed to define the dose-response relation in large animal models. This point is important because statins are reported to exert a double-edged role in angiogenesis signaling.[28] Although such antiangiogenic effects of statins at high dose did not occur in a murine model,[24] this must be examined in large animal models. Second, we only examined the therapeutic effects of a single intramuscular injection of statin-NP. Whether repetitive delivery of statin-NP at an optimal dose over time produces greater therapeutic effects remains to be investigated.

In conclusion, this platform nanotechnology of vascular endothelial cell-selective delivery of statin is a promising strategy toward more effective and integrative nanomedicine in patients with severe organ ischemia, and represents a significant advance in therapeutic neovascularization over current approaches. The nanotechnology platform may be developed further as an "integrative" approach for therapeutic neovascularization, and extended to target other molecular signals specific to vascular endothelial cells.

Acknowledgments

We thank Eiko Iwata and Miho Miyagawa for their technical supports in this study.

Sources of Funding

This study was supported by Grants-in-Aid for Scientific Research (19390216, 19650134) from the Ministry of Education, Science, and Culture, Tokyo, Japan, and by Health Science Research Grants (Research on Translational Research and Nanomedicine) from the Ministry of Health, Labor, and Welfare, Tokyo, Japan.

Disclosures

Dr Egashira holds a patent on the results reported in the present study. The remaining authors report no conflicts.

References

1. Losordo DW, Dimmeler S. Therapeutic angiogenesis and vasculogenesis for ischemic disease. Part I: angiogenic cytokines. *Circulation*. 2004;109:2487–2491.
2. Losordo DW, Dimmeler S. Therapeutic angiogenesis and vasculogenesis for ischemic disease: part II: cell-based therapies. *Circulation*. 2004;109:2692–2697.
3. Baumgartner I, Pieczek A, Manor O, Blair R, Kearney M, Walsh K, Isner JM. Constitutive expression of phVEGF165 after intramuscular gene transfer promotes collateral vessel development in patients with critical limb ischemia. *Circulation*. 1998;97:1114–1123.
4. Marui A, Tabata Y, Kojima S, Yamamoto M, Tambara K, Nishina T, Saji Y, Inui K, Hashida T, Yokoyama S, Onodera R, Ikeda T, Fukushima M, Komeda M. A novel approach to therapeutic angiogenesis for patients with critical limb ischemia by sustained release of basic fibroblast growth factor using biodegradable gelatin hydrogel: an initial report of the phase I-IIa study. *Circ J*. 2007;71:1181–1186.
5. Schaper W, Scholz D. Factors regulating arteriogenesis. *Arterioscler Thromb Vasc Biol*. 2003;23:1143–1151.
6. Heil M, Schaper W. Influence of mechanical, cellular, and molecular factors on collateral artery growth (arteriogenesis). *Circ Res*. 2004;95:449–458.
7. Ferrara N, Alitalo K. Clinical applications of angiogenic growth factors and their inhibitors. *Nat Med*. 1999;5:1359–1364.
8. Carmeliet P, Jain RK. Angiogenesis in cancer and other diseases. *Nature*. 2000;407:249–257.

9. Yonemitsu Y, Kaneda Y, Morishita R, Nakagawa K, Nakashima Y, Sueishi K. Characterization of in vivo gene transfer into the arterial wall mediated by the Sendai virus (hemagglutinating virus of Japan) liposomes: an effective tool for the in vivo study of arterial diseases. *Lab Invest.* 1996;75:313–323.
10. Ohtani K, Egashira K, Hiasa K, Zhao Q, Kitamoto S, Ishibashi M, Usui M, Inoue S, Yonemitsu Y, Sueishi K, Sata M, Shibuya M, Sunagawa K. Blockade of vascular endothelial growth factor suppresses experimental restenosis after intraluminal injury by inhibiting recruitment of monocyte lineage cells. *Circulation.* 2004;110:2444–2452.
11. Zhao Q, Egashira K, Hiasa K, Ishibashi M, Inoue S, Ohtani K, Tan C, Shibuya M, Takeshita A, Sunagawa K. Essential role of vascular endothelial growth factor and Flt-1 signals in neointimal formation after periadventitial injury. *Arterioscler Thromb Vasc Biol.* 2004;24:2284–2289.
12. Zhao Q, Egashira K, Inoue S, Usui M, Kitamoto S, Ni W, Ishibashi M, Hiasa Ki K, Ichiki T, Shibuya M, Takeshita A. Vascular endothelial growth factor is necessary in the development of arteriosclerosis by recruiting/activating monocytes in a rat model of long-term inhibition of nitric oxide synthesis. *Circulation.* 2002;105:1110–1115.
13. Celletti FL, Waugh JM, Amabile PG, Brendolan A, Hilfiker PR, Dake MD. Vascular endothelial growth factor enhances atherosclerotic plaque progression. *Nat Med.* 2001;7:425–429.
14. Kawashima Y, Yamamoto H, Takeuchi H, Hino T, Niwa T. Properties of a peptide containing DL-lactide/glycolide copolymer nanospheres prepared by novel emulsion solvent diffusion methods. *Eur J Pharm Biopharm.* 1998;45:41–48.
15. Panyam J, Zhou WZ, Prabha S, Sahoo SK, Labhasetwar V. Rapid endolysosomal escape of poly(DL-lactide-co-glycolide) nanoparticles: implications for drug and gene delivery. *Faseb J.* 2002;16:1217–1226.
16. Davda J, Labhasetwar V. Characterization of nanoparticle uptake by endothelial cells. *Int J Pharm.* 2002;233:51–59.
17. Takemoto M, Liao JK. Pleiotropic effects of 3-hydroxy-3-methylglutaryl coenzyme a reductase inhibitors. *Arterioscler Thromb Vasc Biol.* 2001; 21:1712–1719.
18. Llevadot J, Murasawa S, Kureishi Y, Uchida S, Masuda H, Kawamoto A, Walsh K, Isner JM, Asahara T. HMG-CoA reductase inhibitor mobilizes bone marrow–derived endothelial progenitor cells. *J Clin Invest.* 2001; 108:399–405.
19. Altieri DC. Statins' benefits begin to sprout. *J Clin Invest.* 2001;108: 365–366.
20. Sata M, Nishimatsu H, Suzuki E, Sugiura S, Yoshizumi M, Ouchi Y, Hirata Y, Nagai R. Endothelial nitric oxide synthase is essential for the HMG-CoA reductase inhibitor cerivastatin to promote collateral growth in response to ischemia. *Faseb J.* 2001;15:2530–2532.
21. Kureishi Y, Luo Z, Shiojima I, Bialik A, Fulton D, Lefer DJ, Sessa WC, Walsh K. The HMG-CoA reductase inhibitor simvastatin activates the protein kinase Akt and promotes angiogenesis in normocholesterolemic animals. *Nat Med.* 2000;6:1004–1010.
22. Kitamoto S, Nakano K, Hirouchi Y, Kohjimoto Y, Kitajima S, Usui M, Inoue S, Egashira K. Cholesterol-lowering independent regression and stabilization of atherosclerotic lesions by pravastatin and by antimonocyte chemoattractant protein-1 therapy in nonhuman primates. *Arterioscler Thromb Vasc Biol.* 2004;24:1522–1528.
23. Ni W, Egashira K, Kataoka C, Kitamoto S, Koyanagi M, Inoue S, Takeshita A. Antiinflammatory and antiarteriosclerotic actions of HMG-CoA reductase inhibitors in a rat model of chronic inhibition of nitric oxide synthesis. *Circ Res.* 2001;89:415–421.
24. Sata M, Nishimatsu H, Osuga J, Tanaka K, Ishizaka N, Ishibashi S, Hirata Y, Nagai R. Statins augment collateral growth in response to ischemia but they do not promote cancer and atherosclerosis. *Hypertension.* 2004;43: 1214–1220.
25. Hiasa K, Ishibashi M, Ohtani K, Inoue S, Zhao Q, Kitamoto S, Sata M, Ichiki T, Takeshita A, Egashira K. Gene transfer of stromal cell-derived factor-1alpha enhances ischemic vasculogenesis and angiogenesis via vascular endothelial growth factor/endothelial nitric oxide synthase-related pathway: next-generation chemokine therapy for therapeutic neovascularization. *Circulation.* 2004;109:2454–2461.
26. Dimmeler S, Aicher A, Vasa M, Mildner-Rihm C, Adler K, Tiemann M, Rutten H, Fichtlscherer S, Martin H, Zeiher AM. HMG-CoA reductase inhibitors (statins) increase endothelial progenitor cells via the PI 3-kinase/Akt pathway. *J Clin Invest.* 2001;108:391–397.
27. Fujii T, Yonemitsu Y, Onimaru M, Tanii M, Nakano T, Egashira K, Takehara T, Inoue M, Hasegawa M, Kuwano H, Sueishi K. Nonendothelial mesenchymal cell-derived MCP-1 is required for FGF-2-mediated therapeutic neovascularization: critical role of the inflammatory/arteriogenic pathway. *Arterioscler Thromb Vasc Biol.* 2006;26: 2483–2489.
28. Urbich C, Dernbach E, Zeiher AM, Dimmeler S. Double-edged role of statins in angiogenesis signaling. *Circ Res.* 2002;90:737–744.

Nanoparticle-Mediated Delivery of Nuclear Factor κB Decoy Into Lungs Ameliorates Monocrotaline-Induced Pulmonary Arterial Hypertension

Satoshi Kimura, Kensuke Egashira, Ling Chen, Kaku Nakano, Eiko Iwata, Miho Miyagawa, Hiroyuki Tsujimoto, Kaori Hara, Ryuichi Morishita, Katsuo Sueishi, Ryuji Tominaga, Kenji Sunagawa

Abstract—Pulmonary arterial hypertension (PAH) is an intractable disease of the small pulmonary artery that involves multiple inflammatory factors. We hypothesized that a redox-sensitive transcription factor, nuclear factor κB (NF-κB), which regulates important inflammatory cytokines, plays a pivotal role in PAH. We investigated the activity of NF-κB in explanted lungs from patients with PAH and in a rat model of PAH. We also examined a nanotechnology-based therapeutic intervention in the rat model. Immunohistochemistry results indicated that the activity of NF-κB increased in small pulmonary arterial lesions and alveolar macrophages in lungs from patients with PAH compared with lungs from control patients. In a rat model of monocrotaline-induced PAH, single intratracheal instillation of polymeric nanoparticles (NPs) resulted in delivery of NPs into lungs for ≤14 days postinstillation. The NP-mediated NF-κB decoy delivery into lungs prevented monocrotaline-induced NF-κB activation. Blockade of NF-κB by NP-mediated delivery of the NF-κB decoy attenuated inflammation and proliferation and, thus, attenuated the development of PAH and pulmonary arterial remodeling induced by monocrotaline. Treatment with the NF-κB decoy NP 3 weeks after monocrotaline injection improved the survival rate as compared with vehicle administration. In conclusion, these data suggest that NF-κB plays a primary role in the pathogenesis of PAH and, thus, represent a new target for therapeutic intervention in PAH. This nanotechnology platform may be developed as a novel molecular approach for treatment of PAH in the future. (***Hypertension.* 2009;53:877-883.**)

Key Words: pulmonary hypertension ■ lung ■ inflammation ■ leukocytes

Pulmonary arterial hypertension (PAH) is an intractable disease of the small pulmonary arteries that results in a progressive increase in pulmonary vascular resistance, right ventricular failure, and, ultimately, premature death.[1–3] Because its mortality remains high even after the introduction of prostacyclin infusion therapy (which has raised the 5-year survival rate to ≈50%), the development of a more effective and less invasive therapy for PAH is urgently needed.

Recent evidence suggests an important role of monocyte chemoattractant protein (MCP) 1–mediated inflammation in the mechanism of PAH.[4–8] However, the therapeutic benefits of MCP-1 blockade were not optimal for clinical application.[5,6] During the inflammatory process of PAH, several inflammatory factors (eg, MCP-1, interleukin [IL] 1, IL-6, and tumor necrosis factor [TNF] α) are overproduced, leading to a vicious circle.[1–3] A redox-sensitive transcription factor, nuclear factor κB (NF-κB), is known to regulate expression of chemokines such as MCP-1 and multiple inflammatory cytokines such as IL-6 and TNF-α. Blockade of NF-κB by transfection of NF-κB "decoy" oligodeoxynucleotides may attenuate the vascular pathology associated with reduced expression of NF-κB–dependent genes.[9–12] However, no previous study has addressed the specific role of the NF-κB pathway in the pathogenesis of PAH. Therefore, we hypothesized that controlled local delivery of NF-κB decoy into lungs, targeting a battery of multiple important inflammatory cytokines, would be a favorable therapeutic approach for PAH. To this end, we have recently developed bioabsorbable polymeric nanoparticles (NPs) formulated from a poly-(ethylene glycol)-*block*-lactide/glycolide copolymer (PEG-PLGA).[13–15]

The primary aim of this study was to investigate the role of the NF-κB pathway in the pathogenesis of PAH. We first examined the activity of NF-κB in patients with PAH. We then used a rat model of monocrotaline (MCT)-induced PAH to examine whether NP-mediated delivery of the NF-κB decoy can attenuate the development of PAH.

Methods

Histopathologic and Immunohistochemical Examination of Human Lungs

Human lung tissue was obtained from autopsy specimens from 4 patients whose deaths were attributed to idiopathic PAH and 2

Received August 10, 2008; first decision August 26, 2008; revision accepted March 2, 2009.

From the Departments of Surgery (S.K., R.T.), Cardiovascular Medicine (K.E., L.C., K.N., E.I., M.M., K. Sunagawa), and Pathology (K. Sueishi), Graduate School of Medical Science, Kyushu University, Fukuoka; Hosokawa Powder Technology Research Institute (H.T., K.H.), Osaka; and Division of Clinical Gene Therapy (R.M.), Osaka University Medical School, Osaka, Japan.

Correspondence to Kensuke Egashira, Department of Cardiovascular Medicine, Graduate School of Medical Science, Kyushu University, 3-1-1, Maidashi, Higashi-ku, Fukuoka 812-8582, Japan. E-mail egashira@cardiol.med.kyushu-u.ac

Hypertension is available at http://hyper.ahajournals.org DOI: 10.1161/HYPERTENSIONAHA.108.121418

patients whose deaths were attributed to nonlung disease (Figure S1, available in the online data supplement at http://hyper.ahajournals.org). Additional details are provided in the online data supplement.

Preparation of NPs

The NF-κB decoy oligodeoxynucleotides labeled with or without fluorescein-isothiocyanate (FITC) were prepared as described previously.[10,11] The decoy is directed against the NF-κB binding site in the promoter region that corresponds with NF-κB–responsive genes and works to inhibit binding of this transcription factor to the promoter region.[10,11] PEG-PLGA NPs encapsulated with FITC, NF-κB decoy, or FITC-labeled NF-κB decoy were prepared using an emulsion solvent diffusion method.[13,14] The average diameter of PEG-PLGA NPs was 44 nm. To measure FITC release kinetics, FITC-NP was immersed in Tris-EDTA buffer, and the released FITC was measured. Additional details are provided in the online data supplement.

In Vivo Experiments With a Rat Model of MCT-Induced PAH

Rats were SC injected with 60 mg/kg of MCT, which induces severe PAH within 3 weeks.[5,16,17] In the prevention protocol, animals were assigned to either an untreated control group or a group that received a single intratracheal instillation of NF-κB decoy alone (50 μg), FITC-NP (1000 μg of PEG-PLGA), or NF-κB decoy NPs (50 μg of NF-κB decoy per 1000 μg of PEG-PLGA) immediately after MCT (n=6 each). For intratracheal instillation, a volume of 0.1 mL of phosphate buffer suspension of NP or NF-κB decoy was injected gently into the trachea of animals accompanied by an equal volume of air. The biodistribution of FITC in the lung was also examined 3, 7, and 14 days after intratracheal instillation of FITC only, FITC-NPs, or FITC-labeled NF-κB decoy NPs in rats injected with MCT. In the treatment protocol, rats were divided into 2 groups (rats treated with a single intratracheal instillation of phosphate buffer and rats treated with NF-κB decoy NPs; n=33 each) 21 days after MCT injection, when severe PAH had been established.

Hemodynamic Measurements

Three weeks after MCT administration, the animals were anesthetized with sodium pentobarbital, and then polyethylene catheters were inserted into the right ventricle (RV) through the jugular vein and the carotid artery for hemodynamic measurements. RV systolic pressure and systemic blood pressure were measured with a polygraph system (AP-601G, Nihon Kohden).[5]

Assessment of Right Heart Hypertrophy and Pulmonary Arterial Remodeling

After systemic arterial and RV pressure had been recorded, the animals were euthanized, and the lungs and heart were isolated. The RV wall was dissected from the left ventricle (LV) and ventricular septum (S). The wet weight of the RV and LV+S was determined, and RV hypertrophy was expressed as follows: RV/(LV+S).[5]

The lungs were perfused with a solution of 10% phosphate buffered formalin (pH 7.4). At the same time, 10% phosphate buffered formalin (pH 7.4) was administered into the lungs via the tracheal tube at a pressure of 20 cm H_2O. These specimens were processed for light microscopy by routine paraffin embedding. The degree of remodeling (muscularization) of the small peripheral pulmonary arteries was assessed by double immunohistochemical staining of the 3-μm sections with an anti–α-smooth muscle actin antibody (dilution 1:500, clone 1A4, Dako) and anti–platelet endothelial cell adhesion molecule 1 (M-20) antibody (dilution 1:100, Santa Cruz Biotechnology) modified from a protocol described elsewhere.[18]

To assess the type of remodeling in the muscular pulmonary arteries, microscopic images were analyzed. In each rat, 30 to 40 intra-acinar arteries were categorized as muscular (ie, with a complete medial coat of muscle), partially muscular (ie, with only a crescent of muscle), or nonmuscular (ie, with no apparent muscle). The arteries were counted and averaged within a range of diameters from 25 to 50 μm.

Histopathologic and Immunohistochemical Analysis

The degrees of monocyte infiltration were evaluated by immunostaining with the ED-1 (analogue of human CD68) antibody against monocytes. For quantification, a blind observer counted the number of ED-1–positive cells in 10 fields.[4] Monocytes were also subjected to immunostaining with antibodies against FITC, an epitope (α-p65) on the p65 subunit of NF-κB, or nonimmune mouse IgG. The α-p65 monoclonal antibody recognizes an epitope on the p65 subunit that is masked by bound inhibitor of κB (I-κB).[9] Therefore, this antibody exclusively detects activated NF-κB.[12]

Electrophoretic Mobility-Shift Assays

Nuclear extracts were prepared from the whole-lung homogenates using a nuclear extract kit (NE-PER Nuclear and Cytoplasmic Extraction Reagents, Thermo Science) according to the manufacturer's instructions. The protein was measured using a BCA Protein Assay kit (Thermo Science). For NF-κB activation, a nonradioactive electrophoresis mobility-shift assay kit (AY1030, Panomics) was used according to the manufacturer's instructions. Five μg of nuclear protein were incubated for 30 minutes at room temperature with a biotinylated oligonucleotide containing the NF-κB binding site, and then the samples were separated on a nondenaturing polyacrylamide gel and blotted onto a positively charged nylon membrane. After blotting, the oligos on the membrane were fixed using a UV cross-linker oven. Then, the membrane was incubated with streptavidin-horseradish-peroxidase solution at room temperature for 15 minutes and with detection reagents for 5 minutes. Nuclear proteins that were bound to the NF-κB binding site were detected by chemiluminescence with the use of the LAS-1000 detection system (Fujifilm).

Real-Time Quantitative RT-PCR

Real-time PCR amplification was performed with the rat cDNA with the use of the ABI PRI8:21 PM 7000 Sequence Detection System (Applied Biosystems), as described previously.[12] TaqMan primer/probes for MCP-1, TNF-α, IL-1, IL-6, intercellular adhesion molecule 1, and GAPDH, which served as the endogenous reference, were purchased from Applied Biosystems (Assay-on-Demand gene expression products Rn00580555, Rn99999017, Rn00580432, Rn00561420, and Rn00564227 and TaqMan Rodent GAPDH Control Reagents, respectively).

Intracellular Delivery of NPs Incorporated With an FITC-Labeled NF-κB Decoy to Human Monocytes and Pulmonary Arterial Smooth Muscle Cells

The human monocyte cell line THP-1 was obtained from the German Collection of Micro-organisms and Cell Cultures and was used between passages 4 and 8. Cells were cultured in RPMI 1640 with 10% FBS in a humidified atmosphere of 5% CO_2 in air. The cell density was adjusted to 10^6 cells per milliliter in 1 mL of serum-free medium in 35-mm-diameter dishes. The cells were serum deprived 24 hours before the experiment. The growth medium was replaced with FITC-conjugated NF-κB decoy encapsulated PEG-PLGA NP suspension medium (0.5 mg/mL) and then further incubated for 1 hour. At the end of the experiment, the cells were washed 3 times with PBS to eliminate excess NPs that were not incorporated into the cells. Then, the cells were fixed with 10% cold methanol, and nuclei were counterstained with propidium iodide. Cellular uptake of FITC-conjugated NF-κB decoy-encapsulated PEG-PLGA NPs was evaluated by fluorescence microscopy.

Human pulmonary artery smooth muscle cells (PASMCs) were obtained from Cambrex Bio Science, Inc, and cultured as described previously. Cells were used between passages 4 and 8. Human PASMCs were seeded on chambered cover glasses and incubated at 37°C/5% CO_2 until the cells were subconfluent. The following treatments were performed in the same manner.

Lipopolysaccharide-Induced Activation of Human Monocytes

Bacterial lipopolysaccharide (serotype 0111:B4; Sigma) was added at 1 μg/mL to the cells as indicated for each experiment. NF-κB decoy at 5 μg/mL, NF-κB decoy-encapsulated NPs containing 0.1 mg/mL of PEG-PLGA NP and 5 μg/mL of NF-κB decoy, or the vehicle alone was added to the wells simultaneously. Four hours later, the cells were washed 3 times with PBS. NF-κB pathway activity was measured using a TransAM NF-κB p65 ELISA-based assay kit (Active Motif). Nuclear extracts of THP-1 were prepared with the NE-PER kit (Pierce) according to the manufacturer's protocol. All of the procedures were carried out at 4°C. Protein concentration was determined by BCA assay, and 20 μg of protein from each sample were used in the assay. Samples were placed along with 30 μL of binding buffer on a 96-well plate to which oligonucleotides containing an NF-κB consensus binding site had been immobilized. Plates were incubated for 1 hour on a shaker. During this time, the activated NF-κB contained in the sample specifically bound to this nucleotide. The plate was then washed, and the NF-κB complex bound to the oligonucleotides was detected using a primary antibody (100 μL diluted 1:1000 in antibody binding buffer for 1 hour) that is directed against the NF-κB p65 subunit. The plate was then washed again, 100 μL of secondary antibody (diluted 1:1000 in antibody binding buffer) conjugated to horseradish peroxidase was added, and the plate was incubated for 1 hour. The plate was washed again, and 100 μL of developing solution were added. The plate was incubated for 4 minutes away from direct light, 100 μL of stop solution were added, and the plate was read using a plate reader at 450 nm.

Human PASMC Proliferation Assay

Human PASMCs were seeded on 96-well culture plates at 1×10^4 cells per well (n=6 per group) in smooth muscle cells–basal medium with 10% FBS. After 24 hours, the cells were starved for 48 hours in serum-free medium to obtain quiescent nondividing cells. After starvation, 10% FBS was added. Also, a concentration of 1 mg/mL of NF-κB decoy only, NF-κB decoy-encapsulated PEG-PLGA NPs (0.05 mg/mL of PEG-PLGA and 1 mg/mL of decoy), or FITC-encapsulated PEG-PLGA NPs was added to each well. Cells were incubated for another 24 hours after addition of 5′-bromo-2′-deoxyuridine. 5′-Bromo-2′-deoxyuridine incorporation was evaluated by an ELISA kit from Calbiochem.

Statistical Analysis

All of the results are expressed as the mean±SEM. Statistical analysis of differences was performed by ANOVA followed by Bonferroni's multiple comparison test. The survival rates were determined by the Kaplan–Meier method. $P<0.05$ was considered statistically significant.

Results

Activation of NF-κB Expression in Patients With PA6H and in MCT-Induced PAH Rats

Localization of NF-κB activation was examined by immunohistochemical studies in lung tissue from patients using the antibody against α-p65.[9] An intense immunoreactivity of α-p65 was noted primarily in alveolar macrophages and to some extent in small pulmonary arterial lesions (mainly in smooth muscle cells in the medium) from 4 patients with PAH (Figure 1A and Figure S1A). This NF-κB activation was associated with positive staining of MCP-1 and IL-6. In contrast, none at all of α-p65 was detected in 2 control patients whose deaths were not attributed to lung disease (Figure S1B).

In MCT-induced PAH rats, activation NF-κB was noted mainly in alveolar macrophages and weakly in pulmonary artery lesions 7 days after MCT administration (Figure 1B and 1C). An electrophoretic mobility-shift assay was performed to detect the DNA binding activity of NF-κB (Figure S2). The binding activity of the lung increased in rats after MCT injection, which peaked on day 3 and decreased on day 7.

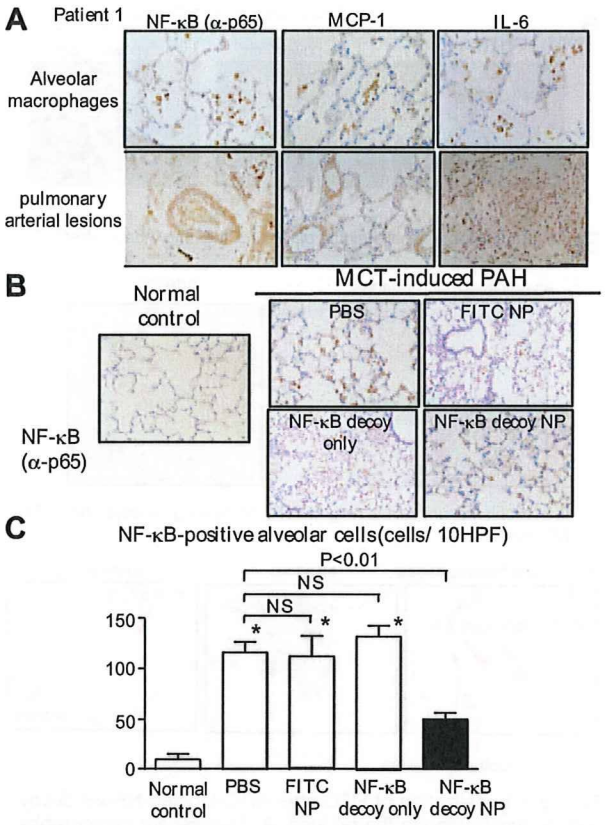

Figure 1. NF-κB activation in patients with PAH and rats with MCT-induced PAH and the effect of intratracheal instillation of NF-κB decoy NPs on NF-κB activation in rats. A, Micrographs of cross sections of the lung from patient 1 stained immunohistochemically with NF-κB (α-p65), MCP-1, and IL-6. Pictures stained with nonimmune IgG control are shown in the inset. Scale bar: 50 μm. B, Micrographs of cross sections of the lung stained immunohistochemically with NF-κB (α-p65) from normal rats and PAH rats 7 days after MCT injection. Scale bar: 50 μm. C, Effects of NF-κB decoy NPs on infiltration of NF-κB (α-p65)–positive cells 7 days after MCT injection. Data are mean±SEM (n=4 each). *$P<0.01$ vs PBS vs normal control.

Effects of Intratracheal Treatment With NF-κB Decoy NP on NF-κB Activation

Single intratracheal instillation of NF-κB decoy NPs, but not FITC NPs or NF-κB decoy only, resulted in marked attenuation of the increased NF-κB (α-p65) activity 7 days after MCT injection (Figure 1B and 1C). Treatment with NF-κB decoy NP markedly attenuated the DNA binding activity of NF-κB after MCT injection (Figure S2).

Because NF-κB was activated in alveolar monocytes and small pulmonary arterial smooth muscle cells in animals and humans with PAH, the effects of NF-κB decoy NPs on NF-κB activity were examined in the human monocyte cell line (THP-1) and in PASMCs in vitro (Figure S3). When those cultured cells were incubated with FITC-labeled NF-κB

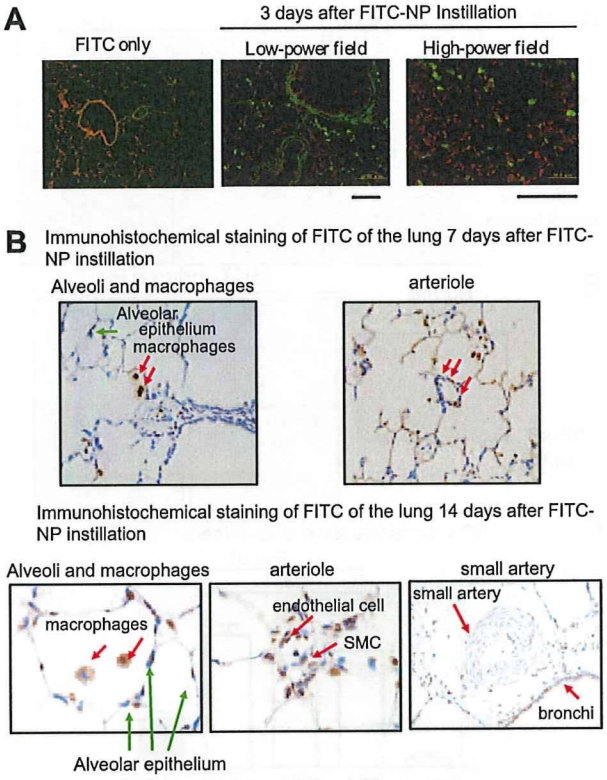

Figure 2. Localization of FITC after FITC-labeled NF-κB decoy NPs postinstillation in the rat lung. A, Fluorescent micrographs of cross sections from lung instillated with FITC only and FITC-labeled NF-κB decoy NPs on day 3 postinstillation. Nuclei were counterstained with propidium iodide (red). Scale bars: 100 μm. B, Micrographs of cross sections stained immunohistochemically against FITC from lung instillated intratracheally with FITC-NPs on days 7 and 14 postinstillation. Scale bars: 100 μm.

decoy NPs for 60 minutes, they were exclusively positive for intracellular localization of FITC. Treatment with NF-κB decoy NPs, but not but with FITC-NPs only or NF-κB decoy only, prevented NF-κB activation in THP-1 cells and attenuated proliferation of human PASMCs.

Localization of FITC-Labeled NF-κB Decoy NPs in the Lung of MCT-Induced PAH

Localization of FITC was examined after a single intratracheal instillation of FITC-labeled NF-κB decoy NPs in animals injected with MCT. Histopathologic examination of lung sections showed that strong FITC signals were detected only in FITC-NP–instillated lung 3 days after instillation, whereas no FITC signals were observed in control noninjected lungs or in lungs injected with FITC only (Figure 2A). There were the FITC-positive cells in bronchi and alveoli, alveolar macrophages, and small arteries. Immunofluorescent staining revealed FITC signals localized mainly in small arteries and arterioles, as well as in small bronchi and alveoli, 7 and 14 days after instillation of FITC-NPs (Figure 2B). FITC signals were not detected in remote organs (liver, spleen, kidney, and heart) on days 1, 3, and 7 (data not shown).

Effects of NF-κB Decoy NP on the Development of PAH in the Rat Model of MCT-Induced PAH

As reported previously by us and by other investigators,[5,16,17] the injection of MCT results in severe PAH (increased RV systolic pressure and RV hypertrophy; Figure 3) associated with small pulmonary arterial remodeling (Figure 4) and increased infiltration of ED-1–positive monocytes (Figure 4) 3 weeks after MCT injection. Single intratracheal treatment with NF-κB decoy NPs but not with NF-κB decoy only or FITC-NPs attenuated the development of PAH (Figure 3), small pulmonary arterial remodeling (Figure 4), and inflammation (Figure 4).

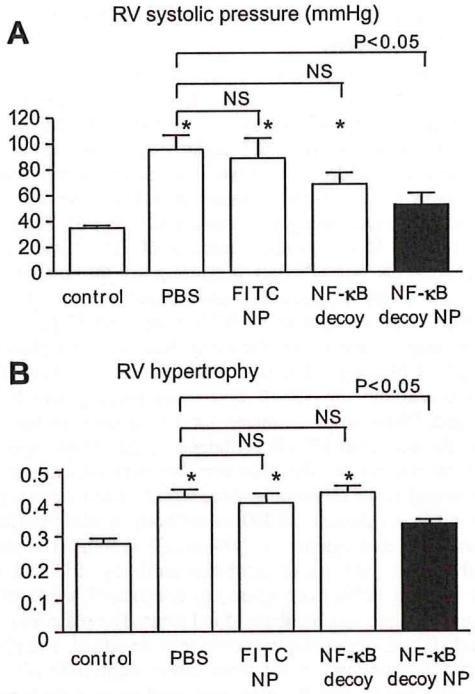

Figure 3. Effects of NF-κB decoy NPs on RV systolic pressure and RV hypertrophy 3 weeks after MCT injection. A, RV systolic pressure 21 days after MCT injection in 4 groups. Data are mean±SEM (n=6 each). *$P<0.05$ vs normal control. B, RV hypertrophy (the ratio of RV/[LV+S]) 21 days after MCT injection in the different treatment groups. Data are mean±SEM (n=6 each). *$P<0.05$ vs normal control.

Effects of NF-κB Decoy NPs on Expression of Proinflammatory Factors

As reported previously,[3,4] MCT-induced PAH was associated with increased gene expression of proinflammatory factors. Treatment with NF-κB decoy NPs significantly reduced the increased gene expression of MCP-1, TNF-α, and IL-1β (Figure 5). NF-κB decoy NPs tended to decrease the expression of IL-6 and intercellular adhesion molecule-1.

In Vitro NP Release Kinetics

An analysis of the in vitro FITC release kinetics from FITC-NP showed an early burst of FITC release such that ≈40% of the total amount ultimately released was present on day 1, followed by sustained release of the remaining FITC over the next 28 days (Figure S4).

Effects of NF-κB Decoy NPs on Survival

Treatment with NF-κB decoy NPs 21 days after MCT injection significantly ($P<0.01$) improved the survival rate (Figure 6).

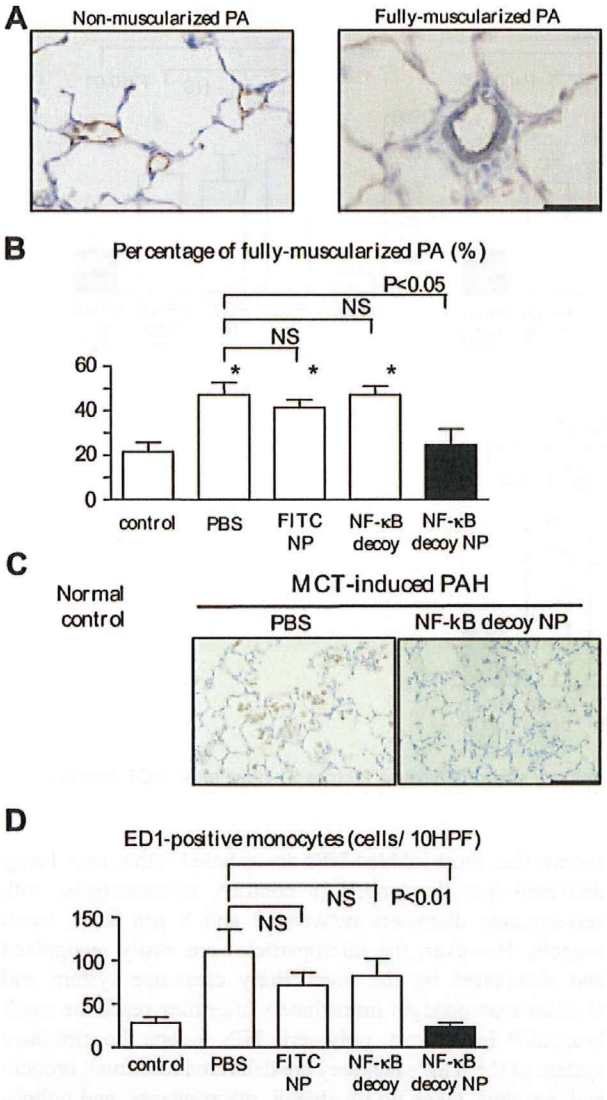

Figure 4. Effects of NF-κB decoy NPs on small pulmonary arterial remodeling and infiltration of monocytes. A, Representative micrographs of nonmuscularized and fully muscularized small pulmonary arteries stained immunohistochemically against the endothelial layer (brown) and medial smooth muscle cells (blue). Scale bar: 50 μm. B, The percentage of fully muscularized small pulmonary arteries in the different treatment groups. Data are mean±SEM (n=6 each). *$P<0.05$ vs normal control. C, Representative micrographs of pulmonary alveoli stained immunohistochemically for ED-1–positive monocytes. Scale bar: 50 μm. D, Infiltration of ED-1–positive monocytes into the lung (the number of positive cells per 10 high-power field cross sections). Data are mean±SEM (n=6 each). *$P<0.01$ vs normal control.

Discussion

The present study demonstrates for the first time that intratracheal instillation of PEG-PLGA NPs is an excellent system for drug delivery of NF-κB decoy to the lung. The FITC signals were detected not only in small bronchial tracts but also in alveolar macrophages and small pulmonary arteries for ≤14 days after a single instillation. After cellular uptake of NPs, NPs might slowly release encapsulated decoy into the cytoplasm as PLGA is hydrolyzed. This might protect the encapsulated decoy from intracellular degradation before its arrival at the nuclear target. Our in vitro studies in cultured human monocytes and pulmonary arterial smooth muscle cells support this notion. Therefore, this platform nanotechnology may represent a novel NP-mediated drug delivery system for treatment of severe lung diseases, including PAH.

The present study also reports a pivotal role of NF-κB in the pathogenesis of PAH. Recently, Sawada et al[19] and Huang et al[20] reported that systemic daily administration of pyrrolidine dithiocarbamate, a nonspecific inhibitor of NF-κB, attenuated the development of MCT-induced PAH. Pyrrolidine dithiocarbamate is known to be a low molecular weight thiol compound and has anti-inflammatory and antioxidant activity independent of the NF-κB pathway. Indeed, in a study by Huang et al,[20] pyrrolidine dithiocarbamate treatment had no effect on MCT-induced NF-κB activation. In contrast, we found in the present study that NF-κB is activated in alveolar macrophages and small pulmonary arteries associated with NF-κB–dependent inflammatory factors (eg, MCP-1, IL-1, and TNF-α) in patients with PAH and rats with MCT-induced PAH, and blockade of NF-κB activation by a single intratracheal instillation of NF-κB decoy NPs reduced inflammatory changes. These data suggest that NF-κB might be pivotal in mediating inflammatory changes seen in PAH.

We also found that intratracheal instillation of NF-κB decoy NPs prevented the development of PAH (increased RV pressure, RV hypertrophy, and pulmonary artery remodeling) in the prevention protocol. We and others have reported that blockade of MCP-1 reduces vascular pathology after vascular injury[9,21–25] and the development of PAH.[5,6] In addition, as we reported in human coronary artery smooth muscle cells in vitro,[12,26] we found that NF-κB decoy NPs attenuated proliferation of human PASMCs in vitro. Therefore, the beneficial effects of NF-κB decoy NPs can be attributable to inhibition of inflammation and smooth muscle cell proliferation resulting from reduced NF-κB activation.

Furthermore, we found that a single intratracheal treatment of NF-κB decoy NPs 3 weeks after MCT injection improved survival rate in the treatment protocol, suggesting that this NP-mediated NF-κB decoy delivery may have significant therapeutic effects. We did not examine the therapeutic effects of repetitive intratracheal instillation of NF-κB decoy NPs, because it is technically difficult to perform multiple intratracheal instillation of this NP system in rats and other small animals. For translation of our present findings into clinical medicine, further studies are needed to investigate whether repetitive delivery of NPs into lungs produces greater therapeutic effects over time.

Several points are worth mentioning with regard to potential clinical applicability. First, from a toxicological point of view, no adverse reactions, eg, pulmonary inflammation, after exposure to a single intratracheal instillation of FITC-NPs (PEG-PLGA at 1 mg per body) or NF-κB decoy NPs (NF-κB decoy at 50 μg per body in rats weighing 250 to 300 g) were noted in the rat model, suggesting that the NPs used in this study may not cause an adverse reaction. However, the 3-week observation period for this NP system might be too short to determine its safety. Second, we reported recently that neither intravenous injection of the NF-κB decoy at 1 mg per body in monkeys nor deployment

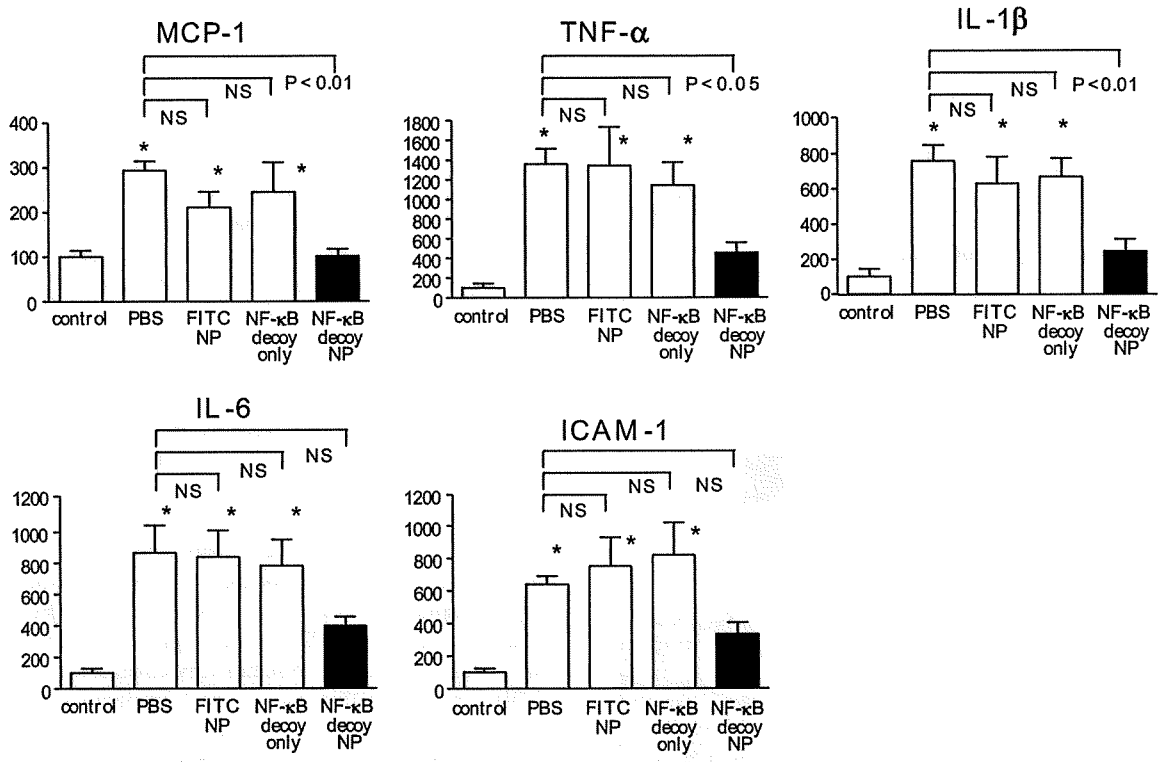

Figure 5. Effects of NF-κB decoy NPs on mRNA levels of various inflammatory and proliferative factors 21 days after MCT injection (n=5 each). *$P<0.01$ vs normal control.

of an NF-κB decoy-eluting stent (≈600 μg per stent) in rabbits showed systemic adverse effects.[12] More important are the findings of a clinical trial that we completed recently to test the feasibility and safety of the NF-κB decoy. The decoy was transfected into the stented coronary artery sites at doses of 1000, 2000, or 4000 μg per body via a channel balloon catheter immediately after successful percutaneous coronary intervention in 18 patients with flow-limiting coronary stenosis.[27] The patients showed low restenosis rates and no evidence of systemic adverse effects during the 6-month observation period. These data support the notion that NF-κB decoy can be applied in a clinical setting. Third, this NP system itself is not suitable for inhalant therapy, because it is known that most inhaled NPs are exhaled rather than being delivered into the lung.[28] In contrast, microparticles with aerodynamic diameters between 2 and 8 μm reach small bronchi. However, the microparticles are easily recognized and eliminated by the mucociliary clearance system and alveolar macrophages immediately after they reach the small bronchi.[28] In contrast, polymeric NPs escape the clearance system of the lung when they are delivered into small bronchi and are, thus, taken up by alveoli, macrophages, and pulmonary small vessels. Therefore, to use this NP system for inhalant therapy, we need to develop the nanocomposite microsized particles[28] that will decompose to NPs after reaching the small bronchi.

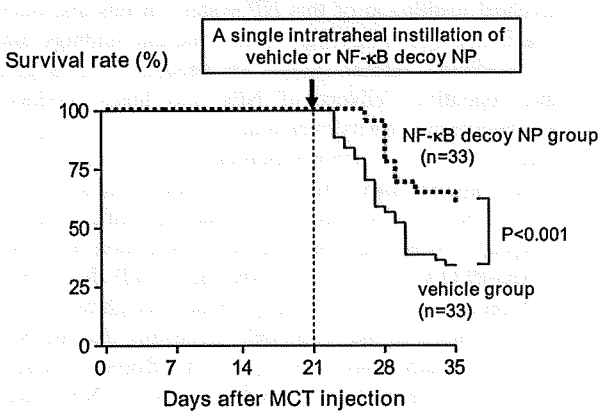

Figure 6. Effects of NF-κB decoy NPs on survival rate. Survival rate analyzed by the Kaplan–Meier method in vehicle and NF-κB decoy NP groups.

Perspectives

This study has shown that NF-κB is activated in pulmonary arterial lesions in patients with PAH and in rats with MCT-induced PAH, and blockade of NF-κB by NP-mediated NF-κB decoy delivery not only prevented the development of MCT-induced PAH in the prevention protocol but also improved survival rate in the treatment protocol. These data support the notion that NF-κB plays a pivotal role in the pathogenesis of PAH and, thus, represents a new therapeutic target for PAH. This nanotechnology platform may be developed as a more effective and less invasive nanomedicine in PAH therapy.

Sources of Funding

This study was supported by Grants-in-Aid for Scientific Research (19390216 and 19650134) from the Ministry of Education, Science, and Culture (Tokyo, Japan) and by Health Science Research grants